Design on a wideband ultra-high birefringence, low dispersion and high nonlinearity photonic crystal fiber with near hyperbolic structure

XUYOU LI, YINGYING YU, BO SUN*, KUNPENG HE
College of Automation, Harbin Engineering University, Harbin, 150001, China

We propose a novel near hyperbolic photonic crystal fiber (PCF). By employing the finite element method, properties of this structure, including the birefringence, dispersion and nonlinearity are investigated. Numerical results show that ultra-high birefringence reaches 5.42×10^{-2}, total dispersion reaches -621.384 ps/nm/km and nonlinear coefficient reaches 100.5 $W^{-1}\cdot km^{-1}$ at $1.55\mu m$ by optimizing structural parameters. Furthermore, birefringence still can reach 10^{-2} at $0.6\mu m$. It can be used potentially as multiple FWM, dispersion compensation, wideband supercontinuum generation, tunable wavelength converters, and ultrashort soliton pulse transmission.

(Received July 10, 2015; accepted October 28, 2015)

Keywords: Fiber design and fabrication; High birefringence; Photonic crystal fibers; Nonlinear optics

1. Introduction

Photonic crystal fiber (PCF) has recently generated great interest in optical sensing and fiber optical communication field thanks to the new ways provided to control and guide light [1, 2], not obtainable with conventional optical fiber. The design of PCF is very flexible. It allows for the various properties including birefringence [3], chromatic dispersion [4] and nonlinearity [5]. The different properties are utilized by various optical equipments. For instance, high birefringent fibers are used to maintain polarization states by reducing polarization coupling in the fiber optic gyroscope (FOG) [6]. The low chromatic dispersion has important applications in designing of dispersion compensation fibers [7]. Supercontinuum (SC) generation is one of the most important applications of the fibers with high nonlinear properties [8]. It is possible to significantly reduce the peak power of SC generation by using the PCF which offers a longer interaction length and a higher effective nonlinearity. By slightly changing the air-hole geometry, it is possible to produce levels of birefringence that exceed the performance of conventional birefringent fiber by an order of magnitude [9-11]. The chromatic dispersion can be controlled and tailored by changing the large index contrast of PCF and the shape, number, and arrangement of air holes [12-15]. The highly nonlinear fibers can be obtained by making large air-holes, or by reducing the core dimension, so that the light is forced into the silica core [16-17]. Although, high birefringence, low chromatic and high nonlinearity have been separately shown in different PCF structures [18-19], there has been little research reported in simultaneously achieving all of these features.

In this paper, we propose a novel near hyperbolic PCF (NH-PCF) which exhibits wideband high birefringence, low chromatic and high nonlinearity in the C band simultaneously. Modal birefringence, chromatic dispersion and nonlinearity have been numerically analyzed by finite element method (FEM) [20-21]. Numerical results show that birefringence of the novel near hyperbolic PCF reaches 5.42×10^{-2}, total dispersion reaches -621.384 ps/nm/km and nonlinear coefficient reaches 100.5 $W^{-1}\cdot km^{-1}$ at $1.55\mu m$ by optimizing structural parameters.

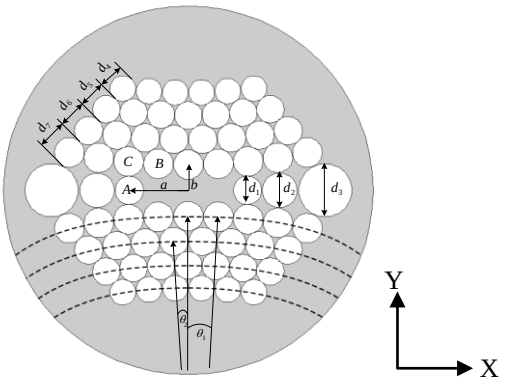

Fig.1. Cross section of the near hyperbolic PCF

2. Structure and Design of near hyperbola PCF

Fig.1 shows the transverse cross section of the near hyperbola PCF with air-hole diameters d_1, d_2, d_3, d_4, d_5, d_6, d_7, core ratio a:b, and angle θ. The proposed structure has four layers air holes (dashed lines) in y-axis direction. The total number of air-holes for rings 1, 2, 3, and 4 are respectively 9, 8, 7, and 6. Angle θ_1 is related to θ_2 by the

relation $\theta_1 = 2\theta_2$. The major axis and minor axis lengths of the fiber core are defined as a and b respectively. In the x-axis direction, the sizes of the three air-holes gradually increase from the innermost to the outermost, and the diameters of them are d_1, d_2, and d_3, respectively. Compared to the traditional PCF, the air-holes arrangement is narrow in the middle and wide ends. It provides wideband high birefringence. The staggered air holes increase the air filling fraction and make the structure more compact to achieve large nonlinearity.

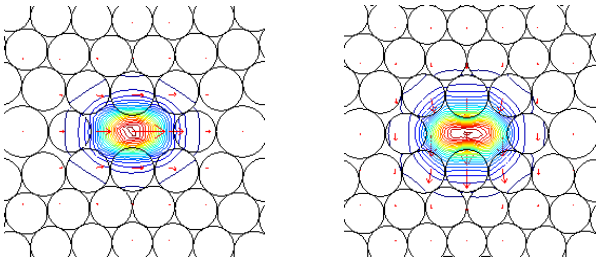

(a) (b)

Fig.2. Field distributions of fundamental modes for (a) x and (b) y polarizations

3. Optical properties of the near hyperbola PCF

The field distributions of fundamental modes for x/y-polarization are shown in Fig.2. The modes are confined well in the fiber core region. It is clearly seen that the profiles of the two modes are distinguishable for the reason that the y-polarized mode has lower air filling fraction than x-polarized.

The modal birefringence, the waveguide dispersion and the nonlinearity can be determined according to the following formulations [22]:

$$B = \frac{\lambda}{2\pi}\left[\beta_x(\lambda) - \beta_y(\lambda)\right] \tag{1}$$

$$D = -\frac{\lambda}{c}\frac{d^2\,\mathrm{Re}\left(n_{eff}\right)}{d\lambda^2} \tag{2}$$

$$\gamma = \frac{2\pi n_2}{\lambda A_{eff}} \tag{3}$$

Where $\beta_x(\lambda)$ and $\beta_y(\lambda)$ are the propagation constants of the x/y-polarized fundamental modes, respectively, $n_2 = 3.0\times10^{-20}\,\mathrm{m^2\cdot W^{-1}}$ is the nonlinear index of silica, A_{eff} is the modal effective area, c is the light velocity in vacuum and λ is the operating wavelength. The total dispersion in a fiber structure can be approximately calculated from [23]:

$$D(\lambda) \approx D_m(\lambda) + D_w(\lambda) \tag{4}$$

where $D_m(\lambda)$ is the material dispersion, which can be obtained through the Sellmeier's equation, and $D_w(\lambda)$ can be calculated from the Eq.(2).

When $\theta_1 = 2\theta_2 = 2.9^\circ$, $d_1 = d_6 = 0.62\mu\mathrm{m}$, $d_2 = 0.76\mu\mathrm{m}$, $d_3 = 1.16\mu\mathrm{m}$, $d_4 = 0.56\mu\mathrm{m}$, $d_5 = 0.6\mu\mathrm{m}$, $d_7 = 0.648\mu\mathrm{m}$ and $a:b = 1.6$, the modal birefringence, total dispersion and nonlinear coefficient of the near hyperbola PCF are shown in Fig. 3. From the Fig. 3(a), we can clearly see that the birefringence of 3.55×10^{-2} is obtained at $1.55\mu\mathrm{m}$. Moreover, the birefringence also can reach a level of 10^{-2} at $0.65\mu\mathrm{m}$. From the Fig. 3(b), we can clearly see that the nonlinear coefficient of $78.671\mathrm{w^{-1}\cdot km^{-1}}$ is achieved at $1.55\mu\mathrm{m}$. From the Fig. 3(c), we can find that the dispersion goes from a positive contribution at shorter wavelengths to a negative contribution at longer wavelengths, and the zero-dispersion is achieved at $0.939\mu\mathrm{m}$. Meantime, the dispersion reaches $-565.366\ \mathrm{ps/nm/km}$ for x-polarization at $1.55\mu\mathrm{m}$. Fig. 3(d) shows the dispersion slope as a function of the wavelength. Within a wavelength range of $0.6\text{-}1.6\mu\mathrm{m}$, the dispersion slope range is -1.1166-0.5628 $\mathrm{ps/nm^2/km}$ for x-polarization, and the zero-slope is obtained at $0.735\mu\mathrm{m}$. These results show that the near hyperbolic PCF has a wideband high birefringence, low dispersion and high nonlinear coefficient. With the further optimization, it can achieve superior performance in the modal birefringence, dispersion and nonlinear coefficient.

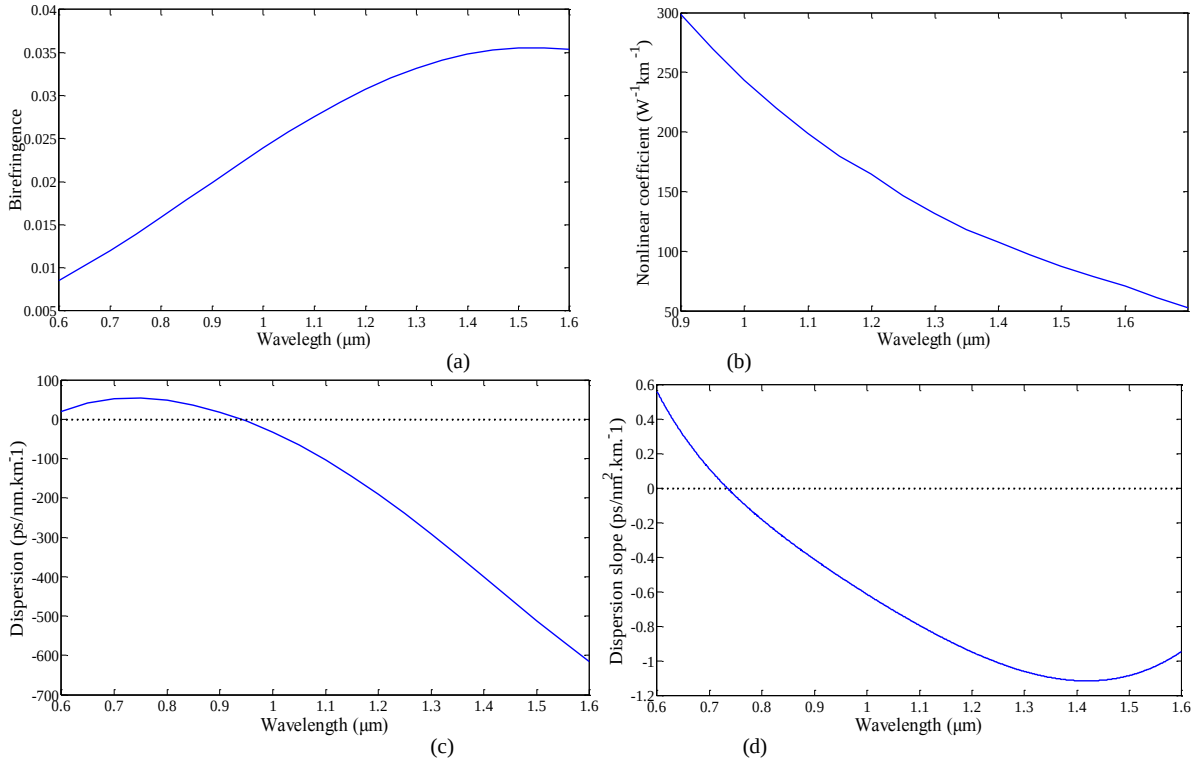

Fig.3. (a) Modal birefringence, (b) nonlinear coefficient, (c) dispersion and (d) dispersion slope as a function of wavelength

4. Influence of the geometric parameters

In this section, when $\theta_1 = 2\theta_2 = 2.9^\circ$, $d_2 = 0.76\mu m$, $d_1 = d_6 = 0.62\mu m$, $d_3 = 1.16\mu m$, $d_4 = 0.56\mu m$, $d_5 = 0.6\mu m$, $d_7 = 0.648\mu m$, we investigate the influences of the core ratio (a:b) on the birefringence, nonlinear coefficient and dispersion. Fig. 4(a) shows the birefringence as a function of the core ratio. From the figure, we can find that the birefringence increases with an increase of core ratio. When a:b=2.5, a maximum birefringence of 0.053 is achieved. Fig. 4(b) shows the nonlinear coefficient as a function of the core ratio. The nonlinear coefficient fluctuates within core ratio range of 1.6-1.9. The reason is that the air filling fraction of the near the core has noticeable change when the air-hole A with fixed diameter moves between air-hole B and C. Within a core ratio range of 1.9-2.5, the nonlinear coefficient shows a downward trend with an increase of core ratio. The influence of the core ratio on the dispersion is shown in Fig. 4(c). We can clearly see that the dispersion first decreases at shorter wavelengths and then increases at longer wavelengths with the increase of core ratio. At $1.55\mu m$, the dispersion are about -246.4, -262.6, -308.6, -381.7. -473.8 $ps/nm/km$ for core ratio a:b=1.7, 1.9, 2.1, 2.3, and 2.5 respectively. When $a:b=1.9$, it has two zero-dispersion wavelengths. When $a:b \geq 2.1$, the values of dispersion are always negative. The influence of the core ratio on the dispersion slope is shown in Fig. 4(d). From the Fig. 4(d), we can find that zero-slope is obtained at $0.739\mu m$, $0.755\mu m$, $0.753\mu m$, $0.766\mu m$ and $0.770\mu m$ as the core ratio a:b changes from 1.7 to 2.5, respectively. From these results, it is clear that a large negative dispersion is obtained, furthermore, it possesses a negative dispersion slope and provide good dispersion compensation.

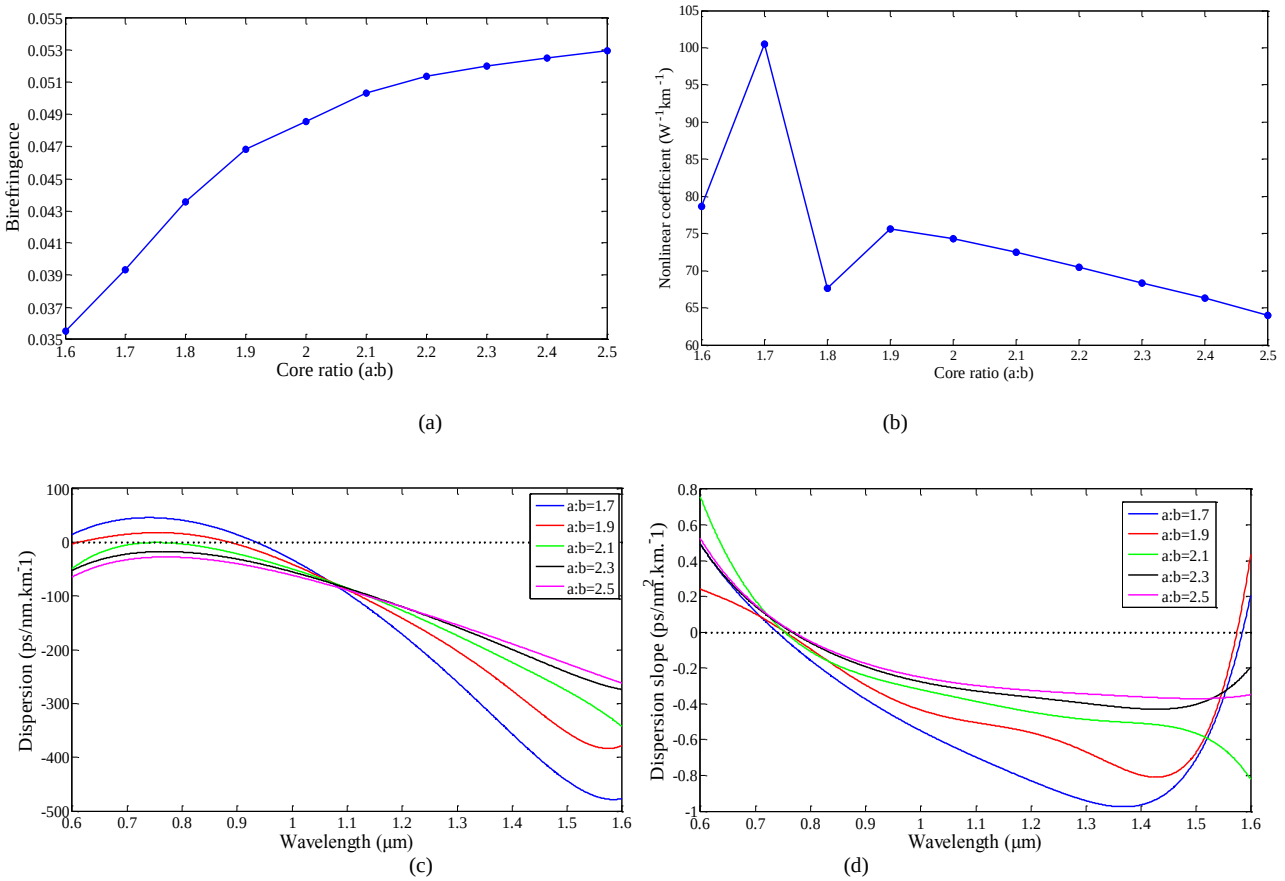

Fig.4. (a) Birefringence and (b) nonlinear coefficient of NH-PCF as a function of core ratio a:b, (c) dispersion and (d) dispersion slope of NH-PCF as a function of wavelength for different core ratio a:b

We then investigate the influence of air-hole diameters on the birefringence, nonlinear coefficient and dispersion. When $\theta_1 = 2\theta_2 = 2.9^\circ$, $d_1 = d_6 = 0.62\mu m$, $d_2 = 0.76\mu m$, $d_3 = 1.16\mu m$, $d_4 = 0.56\mu m$, $d_5 = 0.6\mu m$, $d_7 = 0.648\mu m$ and $a:b = 1.6$. All of the parameters are changed simultaneously by the same proportional coefficient (k). Fig. 5(a) shows the birefringence as a function of the proportional coefficient at $1.55\mu m$. The birefringence first increases and then decreases with an increase of proportional coefficient. When k=1.01, a maximum birefringence of 0.03555 is achieved. Fig. 5(b) shows the nonlinear coefficient as a function of the proportional coefficient at $1.55\mu m$. The nonlinear coefficient increases with an increase of proportional coefficient. The influence of the proportional coefficient on the dispersion is shown in Fig. 5(c). The dispersion decreases with an increase of proportional coefficient toward the longer wavelength. When $k = 0.95$, the value of dispersion is $-621.384\ ps/nm/km$ at $1.55\mu m$. Fig. 5(d) shows the dispersion slope with an increase of wavelength at different proportional coefficients. From the Fig. 5(d), we can clearly see that zero-slope changes with an increase of proportional coefficient. When $k = 0.95$, the dispersion slope lies in (-1.254, 0.75) $ps/nm^2/km$ as the wavelength changes from $0.6\mu m$ to $1.6\mu m$.

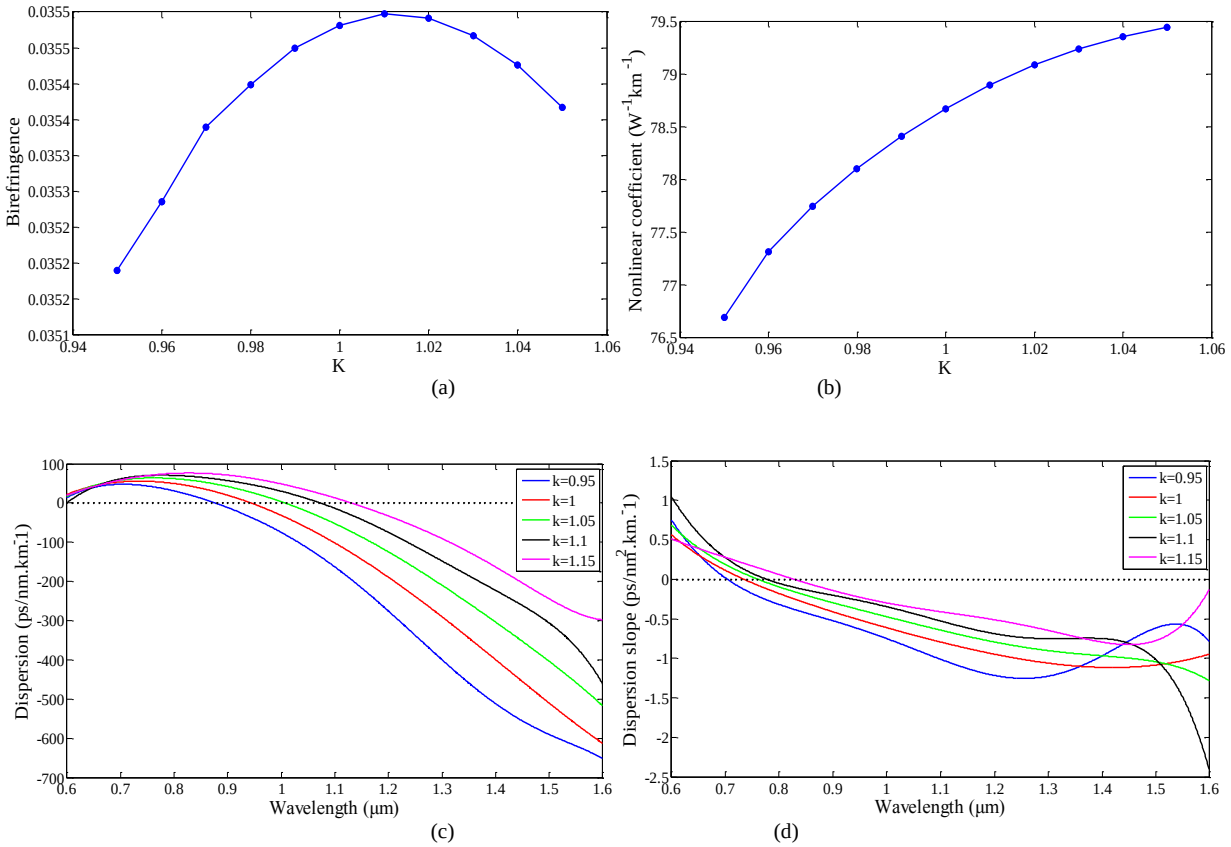

Fig.5. Influence of the proportional coefficient on the (a) birefringence, (b) nonlinear coefficient, (c) dispersion, and (d) dispersion slope

Finally, the influence of d_1 on the birefringence and dispersion are investigated, which are shown in Fig.6. When $\theta_1 = 2\theta_2 = 2.9^\circ$, $d_2 = 0.76\mu m$, $d_3 = 1.16\mu m$, $d_4 = 0.56\mu m$, $d_5 = 0.6\mu m$, $d_7 = 0.648\mu m$, $d_6 = 0.62\mu m$ and $a:b = 1.6$, the modal birefringence, and dispersion as a function of wavelength for the near hyperbola PCF are shown in Fig. 6. Fig. 6(a) shows the influence of d_1 on the birefringence. Obviously, it is found that the birefringence curves present an increasing trending toward a longer wavelength, and the value of birefringence increases with a decrease of d_1 for a specific wavelength. When d_1 =0.56, the value of birefringence is 0.0395 at $1.55\mu m$. Fig. 6(b) shows the dispersion with an increase of wavelength at different d_1 . Notice that the dispersion decreases significantly with the increase of d_1 over the C band. At $1.55\mu m$, the dispersion changes from -563.338 $ps/nm/km$, to -483.645 $ps/nm/km$. The dispersion slope is shown in Fig. 6(c). From the Fig. 6(c), we find that the zero-slope has no significant change with the increase of d_1 .

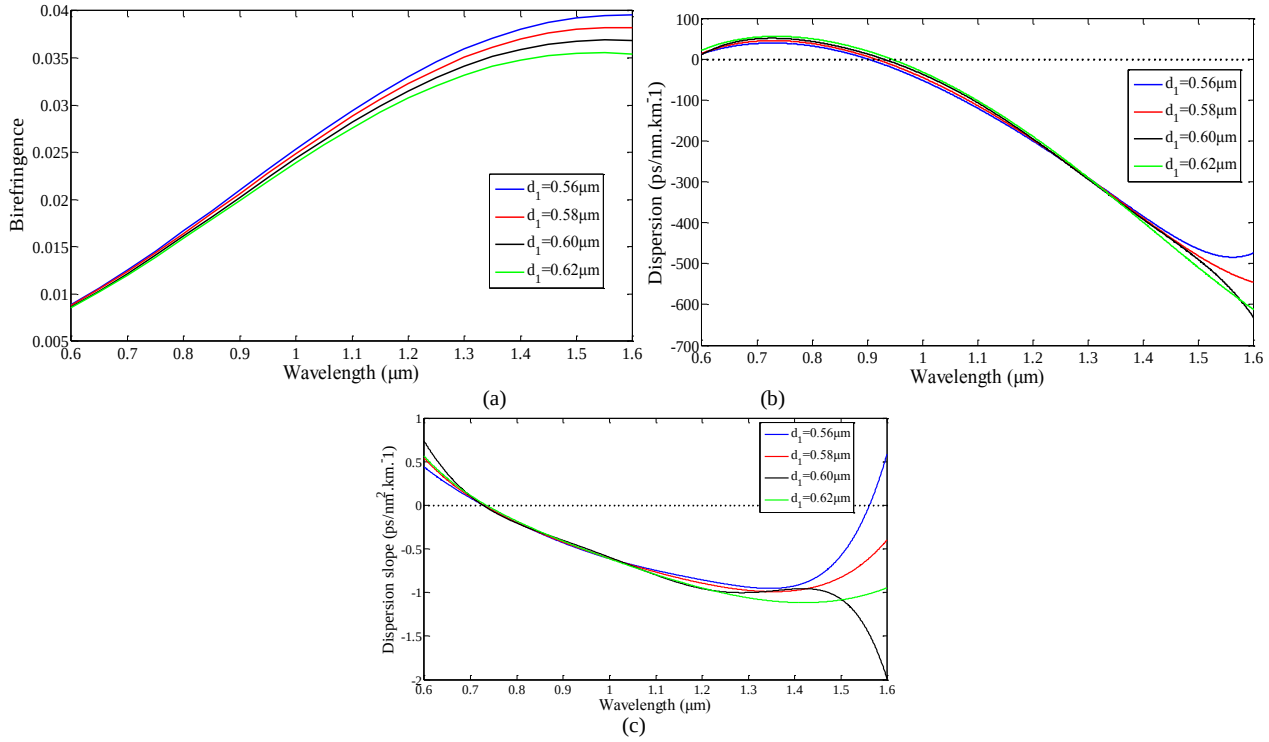

Fig.6. Influence of d_1 on the (a) birefringence, (b) dispersion and (c) dispersion slope.

Table 1. Comparison between properties of the proposed NH-PCF and other various PCFs at 1.55μm.

PCFs	D (ps / nm / km)	B ($\lvert n_x - n_y \rvert$)	γ ($W^{-1} \cdot km^{-1}$)
Ref.[24]	-588.0	1.81×10^{-2}	31.85
Ref.[25]	-257.0	1.85×10^{-2}	-
Ref.[13]	-156	1.94×10^{-2}	-
Ref.[16]	-275	4.2×10^{-2}	3089
NH- PCF	-621.3	5.42×10^{-2}	100.5

Meantime, a comparison is made between properties of the near hyperbola PCF and some other fibers designed. Table 1 compares those fibers taking into account the birefringence, dispersion, and nonlinearity. It clearly indicates that the designed fiber is better for birefringence, dispersion, and nonlinearity (the material of Ref [16] is SF57 glass).

The compact air-holes arrangement of the near hyperbola PCF is narrow in the middle and wide ends. It provides wideband high birefringence, low dispersion and high nonlinearity. We can obtain the wideband high birefringence by increasing the core ratio, decreasing d_1 and optimizing the proportional coefficient. The low dispersion can be obtained by decreasing the core ratio, proportional coefficient and d_1. The high nonlinearity can be obtained by decreasing the core ratio and increasing the proportional coefficient. However, it is also noticed from our viewpoint that the mainly possible technologic difficulties for our proposed PCF are that how to control the angle θ_1 and θ_2 accurately. If it can be solved perfectly in the future, it will be used potentially as multiple FWM, dispersion compensation, wideband supercontinuum generation, tunable wavelength converters, and ultrashort soliton pulse transmission.

5. Conclusions

We have proposed a novel near hyperbolic PCF and investigated its birefringence, dispersion, and nonlinearity properties based on the finite element method. With the proper design, the high birefringence, dispersion, and nonlinear coefficient are up to the value of 5.42×10^{-2}, -621.384 ps / nm / km, and 100.5 $W^{-1} \cdot km^{-1}$ at 1.55μm respectively by optimizing core ratio, proportional coefficient and d_1. Furthermore, the birefringence is still up to the order of 10^{-2} at 0.6μm.

Acknowledgments

The work was supported by the Specific Scientific and Technological Cooperation between China and Russia (Grant No. 2010DFR80140), and the National Natural Science Foundation of China (Grant No. 51309059).

References

[1] P. Russell, Photonic crystal fibers, Science. **299,** 358 (2003).
[2] P. S. J. Russell, Photonic-crystal fibers, J. Lightwave Technol. **24**, 4729 (2006).
[3] J. Ju, W. Jin, M. S. Demokan, Properties of a highly birefringent photonic crystal fiber, IEEE Photon. Technol. Lett. **15**, 1375 (2003).

[4] K. Saitoh, M. Koshiba, T. Hasegawa, E. Sasaoko, Opt. Express **11**, 843 (2003).
[5] J. C. Knight, T. A. Birks, P. St. J. Russell, J. Opt. Soc. Am. A **15,** 748 (1998).
[6] N. Song, P. Ma, J. Jin, J. G. Song, Opt. Fiber. Technol. **18,** 186 (2012).
[7] K. Saitoh, N. Florous, M. Koshiba, Opt. Express **13**, 8365 (2005).
[8] J. M. Dudley, G. Genty, S. Coen, Rev. Mod. Phys. **78,** 1135 (2006).
[9] M. J. Steel, J. R. M. Osgood, Opt. Lett. **26,** 229 (2011).
[10] B. M. A. Rahman, A. K. M. S. Kabir, M. Rajarajan K.T.V. Grattan, Opt. Quant. Electron. **37,** 171 (2005).
[11] B. Hu, M. Lu, W. Li, K.S.Zou, Z. G. Zhou, A. X. Lin N. Li, Appl. Opt. **49,** 6098 (2010).
[12] H. Xu, J. Wu, K. Xu, Y. T. Dai, J.T. Lin, Appl. Opt. **51,** 1021 (2012).
[13] S. E. Kim, B. H. Kim, C. G. Lee, S. J. Lee, K. Oh, C. S. Kee, Opt. Express **20,** 1385 (2012) .
[14] R. Gumenyuk, I. Vartiainen, H. Tuovinen, S. Kivisto, Y. Chamorovskiy, O. G. Okhotnikov, Appl. Opt. **50,** 797 (2011).
[15] S. Kim, C. S. Kee, C. G. Lee, Opt. Express **17,** 7952 (2009).
[16] C. Gui, J. Wang, Large Nonlinearity and Low Dispersion, IEEE Photon. Journal **4,** 2152 (2012).
[17] F. Poli, A. Cucinotta and S. Selleri, Spring Science **102,** 99 (2007) .
[18] S. Ertman, T.R. Wolinski, D. Pysz, R. Buczynski, E. N. Kruszelnicki, R. Dabrowski, Opt. Express **17**, 19298 (2009).
[19] D. Chen, G. Wu, Appl. Opt. **49,** 1682 (2010).
[20] A. Cucinotta, S. Selleri, L. Vincetti, M. Zoboli. IEEE Photon. Technol. Lett. **14,** 1530 (2002).
[21] K. Saitoh, M. Koshiba, IEEE J. Sel. Top. Quant, **38**, 927 (2002).
[22] Y. C. Liu, Y. Lai, Opt. Express **13,** 225 (2004).
[23] K. Saitoh, N. Florous, and M. Koshiba, Opt. Express **13**, 8365 (2005).
[24] S Habib, S Habib, S M Abdur Razzak, A Hossain, Opt. Fiber Technol, **19,** 461 (2013).
[25] W Wang, B Yang, H Song, F Yue, Optik **124,** 2901 (2013).

*Corresponding author: yuyingying58@hotmail.com